(Preprint) AAS 14–347

ORBITAL DENSITY DETERMINATION FROM UNASSOCIATED OBSERVATIONS: UNINFORMATIVE PRIOR AND INITIAL OBSERVATION

Liam M. Healy* **and Christopher Binz***

Unassociated partial-state observations of orbits can provide probabilistic information on the built orbital environment, though traditionally astrodynamicists attempt no analysis of observations until they've been associated. With a large population of small (< 10 cm) objects that could be detected with modern sensors but would still remain unassociated, this is potentially good information that is being ignored. All velocities, within physically defined limits, may be assumed to be equally probable for an observation of an object with position only, and the two together provide complete state information. Orbits can be identified and observations probabilistically associated from an ensemble of unassociated observations from different objects. Such a technique would be an important component of using non-tracking sensors and analysis to compose a time evolution of density in orbit space rather than the traditional approach of composing a histogram of only those objects large and important enough to be tracked and cataloged.

INTRODUCTION

For many years, astrodynamicists have sought to understand the built orbital environment near earth. That is, to understand the distribution and evolution of objects that are present because people put them there, whether they are intact, functioning spacecraft, intact but defunct, fragments of such items, or objects associated with putting satellites into obit, such as rocket bodies. There are several reasons why we pursue this quest. Most significantly, national defense dictates that we know when there is a new launch, especially from countries who will not announce their plans in advance. We also need to be able to use specific spacecraft: communicate with them, dock with them, view them, have them view certain parts of the earth or space, and so on. In recent years, as the debris population has grown, we seek to understand where and what debris presents a hazard to spacecraft, how much of a risk is involved, effective guidance strategies for avoidance, whether there will be and how severe a cascade of collisions (the "Kessler syndrome") due to increasing density will be, and perhaps even how to find densest areas of debris for application of remediation techniques.

At the start of the space era, there was just one orbital object, Sputnik, and the task was to track that object and determine its orbit. As the population grew, the technique expanded. Each object was cataloged, and thus it was possible to find it again for updating the element set. Provisions where made, in the form of uncued sensors, for discovering new objects, but the intent was to associate all observations into tracks, and catalog each of those objects. Astrodynamics is faced with a challenging problem: there are almost no sensing technologies that give full state equivalence in one

*Code 8233, Naval Research Laboratory, Washington, DC 20375-5355.

observation (three position and three momenta to solve a three degree of freedom second order ordinary differential equation). Therefore, the navigation fix cannot be obtained without association, but then there is potential combinatorial confusion in associating the observations. As the catalog has grown into the thousands and tens of thousands, with prospects, given future sensing capabilities of smaller objects, into the hundreds of thousands or even millions of objects, the combined association and partial state equivalence observation problem becomes much harder.

The prospect of a large number of objects together with a lack of full observability suggests another approach to help achieve the goals. Uncertain information can be valuable, and this is even true if the uncertainty is large. Uncertainties are commonly expressed as probability density functions (PDFs), and common astrodynamics analysis, e.g. least squares, assumes normal distributions with small variance. However, in probability and statistics, probabilistic inference techniques have shown the value of techniques that can work with more general distributions. Chief among these is Bayesian statistics.

POSTERIORS FROM A SINGLE OBSERVATION

Complete velocity uncertainty

A single observation of a satellite is usually equivalent to less than the full state. For example, the position vector includes no velocity information. A traditional approach would view the problem as under-determined and no one would attempt to solve it without other (associated) observation(s), at which point one of the standard initial orbit determination methods (e.g., a Lambert solution) would be applied. Our approach allows solution with a single observation, treating the missing information as an uncertainty. This uncertainty needs a distribution as manifested by a probability density function (PDF). Typical PDFs that astrodynamicists are accustomed to are normal (Gaussian); in the present usage, they are most certainly not normal. In fact, we shall invoke the *principle of indifference* [1, p. 40] which provides a non-informative prior. This principle states that, lacking in any other information, we distribute the possible values uniformly. For continuous variables, this can be ambiguous; uniform in one coordinate system (e.g. rectangular) is not uniform in another (e.g. polar). Nevertheless, arguments about uniformity based on reasonable assumptions of observation and physical characteristics of orbits and observation can be made that are plausible to practitioners in the field.

In these calculations, it is important to distinguish ordinary from random variables. A random variable is actually a function, as represented by its PDF. This is written $\Pr_X(x|I)$, meaning the probability density as a function of x, a value of the random variable X, assuming the condition(s) I hold. An ordinary, or *sure*, variable in these expressions is used as in conventional algorithms. This will include observation variables that are assumed known and thus become part of the conditions I. Note particularly that for the purposes of this paper, observations that are made are assumed to be made with complete certainty, which of course is not realistic and is contravention of the usual probabilistic analysis in astrodynamics, where all uncertainty arises to due to either lack of precise observation (noise in instrument) or sometimes lack of complete motion or observation model (so-called "process noise"). A comprehensive approach would include both these uncertainties, and those arising from absent measurement.

In order to get a probability from a density, it is necessary to integrate functions. At the least, confirming that a probability density integrates to 1 is important. Integrals can be computed analytically or numerically; many of the univariate integrals encountered here can be computed analytically (a

computation that is helped by using a computer algebra tool like Maxima[2]). Weisman, Majji, and Alfriend in two papers[3,4] have used the change of variables technique to address the associated observation problem. Those that cannot be computed analytically must be computed numerically, which can be more time consuming. The authors of this paper have another[5] in this conference that show a parallel approach treating observation uncertainty in the associated observation problem.

The single observation considered here is the position vector of the satellite, $\boldsymbol{r}$, which may be conveniently represented in spherical polar coordinates as a geocentric distance, right ascension, and declination. The uncertainty is the entire velocity vector, being completely unknown, and the particular uninformative prior from the principle of indifference will be explained and justified in the following sections. While it appears that there will be a three-dimensional PDF, it turns out that the equations decouple so that dimensionality is reduced; in fact the inclination is univariate and the right ascension of the ascending node is bivariate.

A satellite with a known position vector can have any velocity, within some constraints. The angular momentum direction $\hat{\boldsymbol{h}}$ is constrained to be perpendicular to the direction $\hat{\boldsymbol{r}}$, and so can be chosen from points on the circle S^1. The indifference principle is applied to say that all directions on the circle are equally probable with density $1/2\pi$. With the orbital plane thus defined (normal to $\hat{\boldsymbol{h}}$), the eccentricity vector is chosen with the following constraints: First, the orbit is presumed to be bound $e < 1$, on the assumption that unbound orbits, while possible, are not only rare, but more importantly, do not recur, so that there is no future concern for that object in the near-earth environment. Second, collision orbits, for which perigee is below the surface of the earth, are likewise of limited interest because of their similar rarity and lack of recurrence. These make for a more complicated constraint on the eccentricity vector than on the angular momentum direction.

Once the complete state is specified, the orbital elements may be computed, but it is possible to relate specific elements to components of the position vector in spherical coordinates. With the orbital plane known from the angular momentum direction, the inclination i and right ascension of the ascending node (RAAN) Ω may be determined. In fact, only the declination is needed to find the inclination; both declination and right ascension are needed to find RAAN. Thus an angles-only observation can be used to find i and Ω. With the eccentricity vector $\boldsymbol{e}$ chosen, the semilatus rectum p is computed from the vector's magnitude e and the true anomaly θ, the angle between the known position vector and the eccentricity vector.

In the remainder of this section, each of these elements is computed as a PDF. In essence, a simple sure variable relationship commonly known in spherical trigonometry or orbital mechanics is turned into a PDF.

Inclination

The relationship between inclination i and azimuth A (compass heading) of the velocity vector at the point of observation comes from spherical trigonometry and depends on the declination of the position vector $\hat{\boldsymbol{r}}$, δ; see Figure 1

$$\cos i = \sin A \cos \delta \tag{1}$$

which is valid for the range of angles

$$\delta < i < \pi - \delta. \tag{2}$$

It is used in the launch site-inclination relation [6, p. 324]. Note that there are two values of the azimuth, A and $2\pi - A$, that give the same value of i; there will a double contribution in the inverse

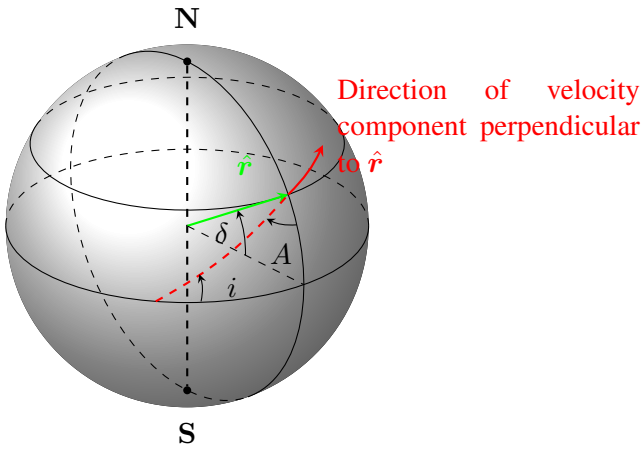

Figure 1. Angle definitions on celestial sphere for satellite with known declination δ and unknown direction of flight A (measured clockwise from North).

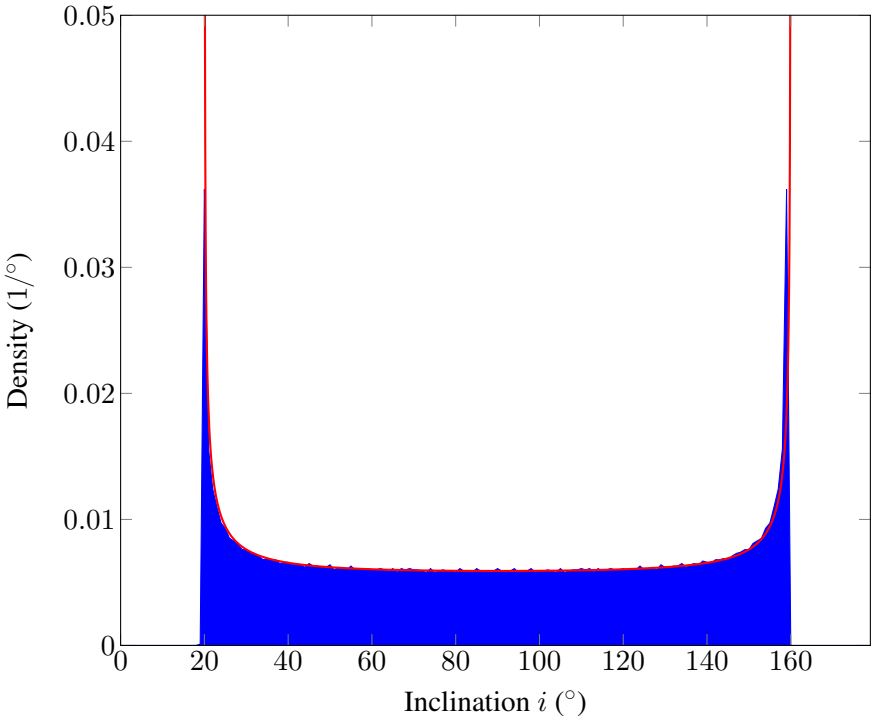

Figure 2. Distribution of inclination from point at declination $\delta = 20°$.

image values. From a probabilistic point of view, this is a change of variables from A to i, because A is the random variable and the inclination is the random variable of interest. The declination of the observation is a known sure variable. From the change of variables formula (40)

$$\left|\frac{dA}{di}\right| = \left|-\frac{\sin i}{\cos\delta\,\cos A}\right| = \frac{\sin i}{\cos\delta\,\cos A}. \tag{3}$$

A substitution will eliminate the dependence on azimuth; from (1),

$$\cos A = \sqrt{1 - \left(\frac{\cos i}{\cos\delta}\right)^2}. \tag{4}$$

In accordance with the principle of indifference, assume a uniform distribution over A, so that $\Pr(A) = 1/2\pi$, so

$$\Pr(i|\delta) = 2\Pr(A)\left|\frac{dA}{di}\right| = \begin{cases} \dfrac{1}{\pi}\dfrac{\sin i}{\sqrt{\cos^2\delta - \cos^2 i}} & \text{if } \delta < i < \pi - \delta, \\ 0 & \text{otherwise.} \end{cases} \tag{5}$$

This probability density function is plotted for a declination of $\delta = 20^\circ$ in Figure 2 (red line), together with a Monte Carlo sample of (1) over 4000 points in A (blue fill). Note that the inclination is dependent only on the declination of the observation point, so an angles-only sensor is sufficient for this element.

The cumulative distribution function (CDF), or indefinite integral of the inclination PDF (5) gives the probability mass of the interval of inclinations,

$$P(i) = \int \Pr(i)\,di = \begin{cases} 0 & i < \delta \\ \dfrac{1}{2} - \dfrac{1}{\pi}\arcsin\left(\dfrac{\cos i}{\cos\delta}\right) & \delta < i < \pi - \delta \\ 1 & \pi - \delta < i. \end{cases} \tag{6}$$

The probability that an inclination lies between two values i_1 and i_2 is the difference $P(i_2) - P(i_1)$.

Right ascension of the ascending node

The right ascension of the ascending node Ω is also related to azimuth through another spherical trigonometric relationship, used in launch timing. [6, p. 325] In the present case, the angle of interest λ, the *auxiliary angle*, is the difference between the right ascension of the satellite α at the observation point $\boldsymbol{r}$ and the right ascension of the ascending node,

$$\lambda = \alpha - \Omega. \tag{7}$$

The auxiliary angle has a range over the full circle, $-\pi < \lambda \leqslant \pi$. The spherical trigonometry relation between the angles can be understood from Figure 3 and substitution for the sine of the inclination from (1) gives

$$\cos\lambda = \frac{\cos A}{\sin i} = \frac{\cos A}{\sqrt{1 - \sin^2 A\cos^2\delta}}, \tag{8}$$

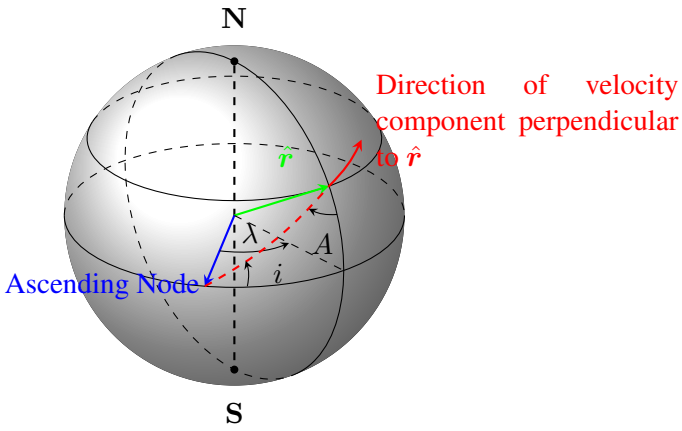

Figure 3. Relationship of auxiliary angle, flight azimuth, and inclination.

and the half-plane (upper or lower) of λ is determined from the half-plane of A. Thus the change of variables from A to λ defines the function g,

$$\lambda = g(A) = \arccos\left(\frac{\cos A}{\sqrt{1-\sin^2 A\cos^2\delta}}\right). \tag{9}$$

To solve the PDF transformation (40), this must be inverted, which can be solved algebraically from (8)

$$\cos A = \frac{\cos\lambda\sin\delta}{\sqrt{1-\cos^2\lambda\cos^2\delta}}; \tag{10}$$

the azimuth as a function of the auxiliary angle

$$A = g^{-1}(\lambda) = \operatorname{sgn}\lambda\arccos\left(\frac{\cos\lambda\sin\delta}{\sqrt{1-\cos^2\lambda\cos^2\delta}}\right), \tag{11}$$

where sgn gives the sign of its argument (± 1), and is present to insure that the half-plane for λ is the same as for A. The derivative of azimuth with respect to auxiliary angle is

$$\frac{dA}{d\lambda} = \frac{\sin\delta}{1-\cos^2\lambda\cos^2\delta}. \tag{12}$$

The variable change formula (40) requires the sum over all values of A that give the same value for λ; in this case, there is only one because A ranges over the full circle. With $Y = \lambda$ and $X = A$, the PDF is

$$\Pr(\lambda|\delta) = \frac{1}{2\pi}\frac{\sin\delta}{(1-\cos^2\lambda\cos^2\delta)}, \tag{13}$$

where the azimuth is equally distributed over all angles, $P(A) = 1/2\pi$. This PDF may be integrated analytically to obtain the cumulative distribution function (CDF),

$$\frac{1}{2\pi}\int\frac{\sin\delta}{(1-\cos^2\lambda\cos^2\delta)}d\lambda = \frac{1}{2\pi}\arctan\left(\frac{\tan\lambda}{\sin\delta}\right). \tag{14}$$

The limits of the auxiliary angle are $-\pi \leqslant \lambda \leqslant \pi$, so the integral over the whole range is one.

In summary, the probability density function of RAAN is a function of the right ascension α and declination δ of the observation,

$$\Pr(\Omega|\alpha,\delta) = \frac{1}{2\pi}\frac{\sin\delta}{1-\cos^2(\Omega-\alpha)\cos^2\delta}. \tag{15}$$

This probability density function is plotted for a declination of $\delta = 20^\circ$ in Figure 4 (red line), together with a Monte Carlo sample of (8) over 4000 points in A (blue fill).

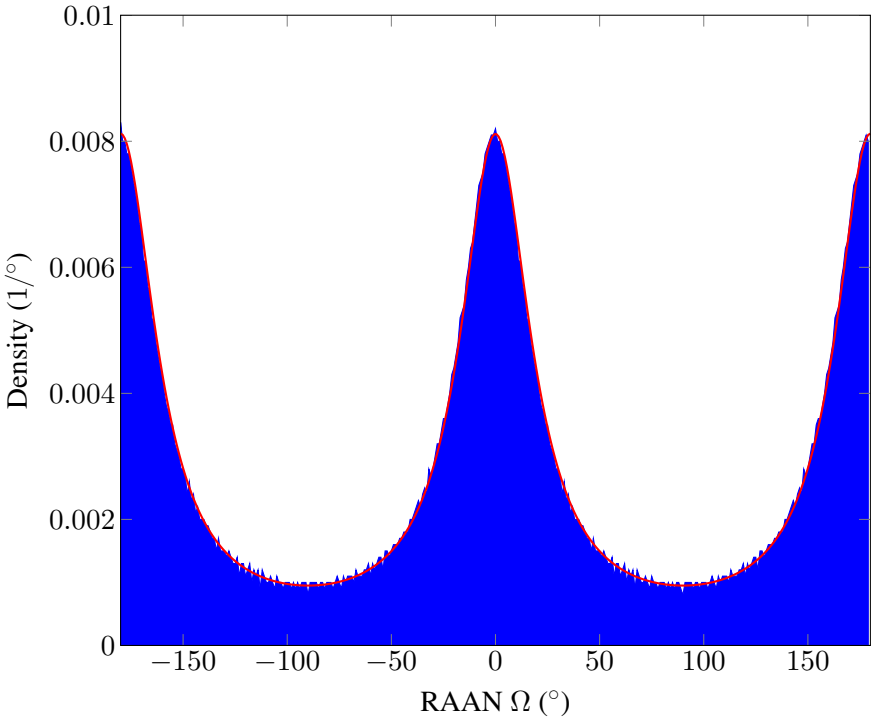

Figure 4. Density of RAAN from single observation $\alpha = 0$, $\delta = 20^\circ$.

Note that the RAAN is dependent only on the right ascension and declination of the observation point, so once again, an angles-only sensor is sufficient for this element.

Semilatus rectum

There are two constraints on the eccentricity vector: the orbit must be bound and must not collide with the earth. These must be taken into account in computing the PDF of the semilatus rectum p and other elements describing the motion in the orbital plane. The collision constraint says that the perigee radius is larger than the radius of the earth $r_p > R_\oplus$ in order to avoid collision. The perigee radius r_p must be larger than the radius of the earth,

$$r_p = a(1-e) = \frac{p}{1+e} = \frac{r + \boldsymbol{r}\cdot\boldsymbol{e}}{1+e} = r\frac{1+e\cos\theta}{1+e} > R_\oplus \tag{16}$$

for true anomaly θ and eccentricity e, or

$$\frac{1+e\cos\theta}{1+e} > \frac{R_\oplus}{r} = \xi, \tag{17}$$

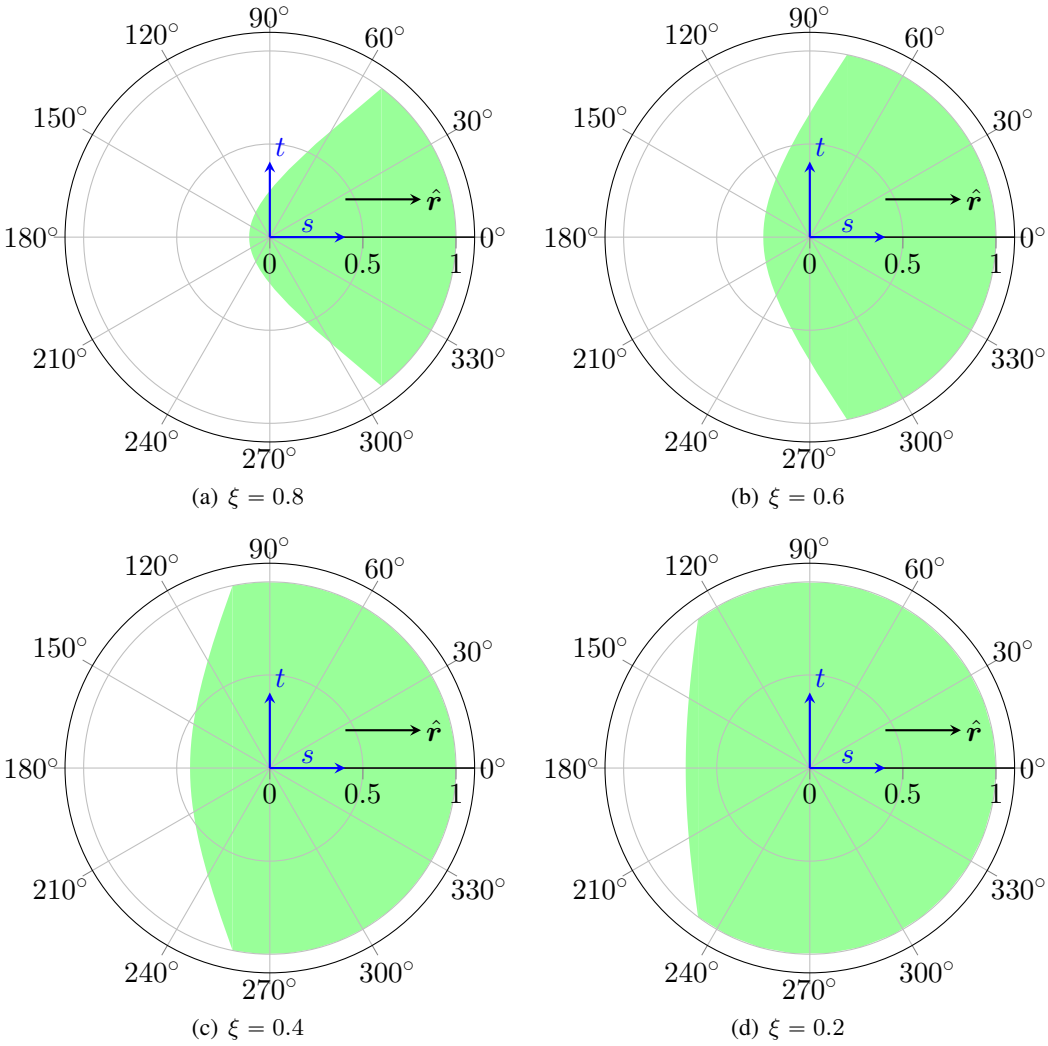

(a) $\xi = 0.8$ (b) $\xi = 0.6$

(c) $\xi = 0.4$ (d) $\xi = 0.2$

Figure 5. Polar plots of permissible eccentricity vector values for varying values of $\xi = R_\oplus/r$. Radius is eccentricity and angle is negative true anomaly.

defining $\xi = R_\oplus/r < 1$ as the ratio of the earth radius to the geocentric distance of the observed point. The maximum eccentricity as a function of true anomaly is therefore given by the relation

$$e_{\text{max}} = \begin{cases} 1 & \text{if } \theta \leqslant \arccos(2\xi - 1), \\ \dfrac{1-\xi}{\xi - \cos\theta} & \text{otherwise.} \end{cases} \tag{18}$$

The allowed values of the eccentricity vector for various ξ are shown in Figure 5 for various values of the radii ratio ξ. In this figure, $\hat{\boldsymbol{r}}$ points to the right, the angle from that axis is the negative of the true anomaly, and the radial magnitude is the eccentricity. The circular arc on the right boundary of the region is the bounded orbit constraint given by the first clause in (18), and the left boundary is the collision constraint given by the second clause. For a sufficiently small true anomaly, any eccentricity over the accepted range ($0 \leqslant e < 1$) is permitted, but if the true anomaly is larger, the collision constraint limits possible eccentricities to lower values than 1.

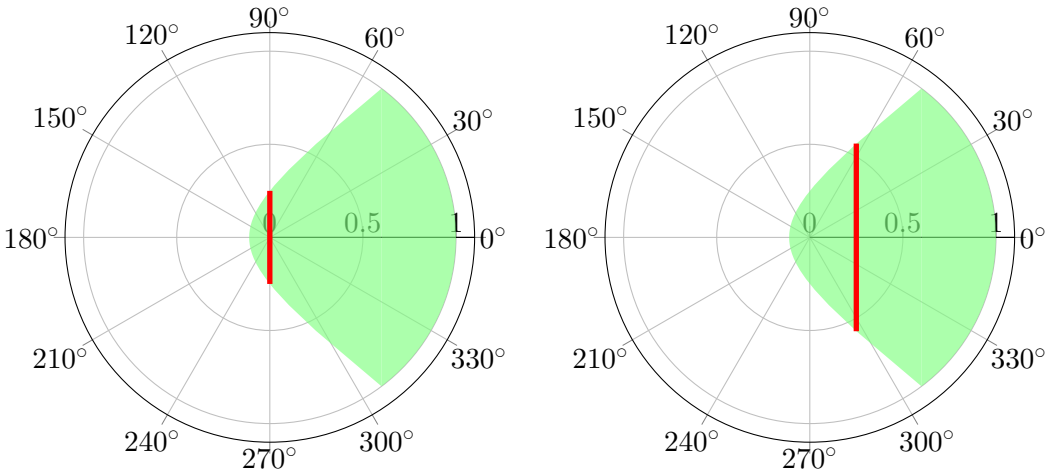

(a) $e\cos\theta = 0$ (b) $e\cos\theta = 0.25$

(c) $e\cos\theta = 0.5$ (d) $e\cos\theta = 0.75$

Figure 6. Probability density $\Pr(e\cos\theta)$ is proportional to the length of the vertical line with constant $s = e\cos\theta$ in the permissible region.

The semilatus rectum p is defined using the two random variables $e \in [0, 1]$ and $\theta \in [-\pi, \pi]$,

$$p = r(1 + e\cos\theta), \tag{19}$$

with the geocentric distance of the observation r a known sure variable. The sum and multiplication by r are an affine transformation, and will be treated later with a known technique. The Cartesian component along the direction of $\hat{\boldsymbol{r}}$, $s = e\cos\theta$, is a function of two random variables that are the remaining part of the semilatus rectum calculation,

$$s = g(e, \theta) = e\cos\theta. \tag{20}$$

Note that variables here are very closely related to three variables of the modified equinoctial elements[7] as used in the associated observation angles-only study.[5] The principle of indifference, which applied to continuous multivariate problems, is ambiguous because a density function constant in one coordinate system, e.g. polar coordinates, is not necessarily constant in another, say rectangular coordinates. The only known value of the PDF is that any value of $\boldsymbol{e}$ that violates the constraint (18) has probability density zero. Since the product of e and $\cos\theta$ is both one Cartesian component and an easy affine transformation into the element p, we shall use a Cartesian flat distribution within the permissible region of the eccentricity vector. That means the density of $e\cos\theta$ is obtained by marginalizing (integrating) the (Cartesian constant) $\boldsymbol{e}$ PDF and is thus proportional to the length of the line between the constraint bounds perpendicular to the horizontal axis; see Figure 6.

In the Cartesian variables $s = e_{\max}\cos\theta$ and $t = e_{\max}\sin\theta$, the Cartesian coordinates along the horizontal and vertical axis of Figure 5. First, eliminate the polar angle θ from the collision constraint limit

$$e_{\max} = \frac{1 - \xi}{\xi - \cos\theta}; \tag{21}$$

setting this value of e in s,

$$s = e_{\max}\cos\theta = \frac{1 - \xi}{\xi - \cos\theta}\cos\theta \tag{22}$$

and solving for $\cos\theta$,

$$\cos\theta = \frac{s\xi}{1 - \xi + s}, \tag{23}$$

the radial distance to the curve (21) can be written in terms of the Cartesian variable s,

$$e_{\max} = \frac{1 - \xi + s}{\xi}. \tag{24}$$

Substituting $t = \sqrt{e_{\max}^2 - s^2}$ results in the Cartesian parameterization of the collision constraint curve,

$$t = \sqrt{\left(\frac{1 - \xi + s}{\xi}\right)^2 - s^2}. \tag{25}$$

Between the minimum and maximum values of s, the value of t may range $-t_{\lim} \leqslant t \leqslant t_{\lim}$,

$$t_{\lim} = \begin{cases} \sqrt{\left(\dfrac{1 - \xi + s}{\xi}\right)^2 - s^2} & \text{if } -\dfrac{1 - \xi}{1 + \xi} \leqslant s \leqslant 2\xi - 1 \\ \sqrt{1 - s^2} & \text{if } 2\xi - 1 \leqslant s \leqslant 1. \end{cases} \tag{26}$$

The probability density function $\Pr(e\cos\theta)$ is proportional to t_{lim}, determined from all values of the eccentricity vector that have the same s. This function is divided by the integral to find the probability density. The integral over s in the crash constraint region is

$$\begin{aligned} I_1 &= \int_{-\frac{1-\xi}{1+\xi}}^{2\xi-1} t_{\text{lim}}\, ds \\ &= \frac{\left(2\,\xi^2+3\,\xi+1\right)\,\sqrt{4\,\xi^3-4\,\xi^4}-\xi\,\sqrt{1-\xi^2}\,\log\left(\frac{2\sqrt{1-\xi^2}\,\sqrt{4\,\xi^3-4\,\xi^4}-4\,\xi^3+2\,\xi^2+2\,\xi}{\xi^2}\right)}{2\,\xi^2+4\,\xi+2} \\ &\qquad + \frac{\xi\,\sqrt{1-\xi^2}\,\log\left(-\frac{2\,\xi-2}{\xi}\right)}{2\,\xi^2+4\,\xi+2} \end{aligned} \tag{27}$$

and in the bound orbit region

$$I_2 = \int_{2\xi-1}^{1} t_{\text{lim}}\, ds = \frac{\pi}{4} - \frac{\arcsin\left(2\,\xi-1\right)+\left(2\,\xi-1\right)\,\sqrt{4\,\xi-4\,\xi^2}}{2}, \tag{28}$$

so the PDF is

$$\Pr_S(e\cos\theta) = \Pr_S(s) = \begin{cases} \dfrac{1}{I_1+I_2}\sqrt{\left(\dfrac{1-\xi+s}{\xi}\right)^2 - s^2} & \text{if } -\dfrac{1-\xi}{1+\xi} \leqslant s \leqslant 2\xi-1 \\ \dfrac{1}{I_1+I_2}\sqrt{1-s^2} & \text{if } 2\xi-1 \leqslant s \leqslant 1. \end{cases} \tag{29}$$

The probability density of the semilatus rectum is an affine transformation [8, p. 44] of that of $e\cos\theta$;

$$p = r(1+e\cos\theta) \tag{30}$$

so

$$\Pr_P(p) = \frac{\xi}{R_\oplus}\Pr_S\left(\frac{p\xi}{R_\oplus}-1\right). \tag{31}$$

An example is plotted in Figure 7. Note that the maximum density is significantly larger than the observed geocentric distance.

Unlike the inclination and right ascension of the ascending node cases, a flat prior in Cartesian eccentricity vector does not have justification on a physical basis. Rather, it could be argued that probability of observation is equal by time. For example, of two possible orbits, the relative probability of observation is proportional to the time spent in the field of view of the sensor. By this standard, the PDF of Figure 7 would look different, and would not just trace out the boundary of the permissible region.

MULTIPLE OBSERVATIONS

Observations of one or more objects

What can be inferred probabilistically about the orbital environment given a sensor whose location observations are unassociated? Assuming first that a single object is observed many times, it is possible to sum the observations and construct a PDF of a particular orbital element. In the limit of

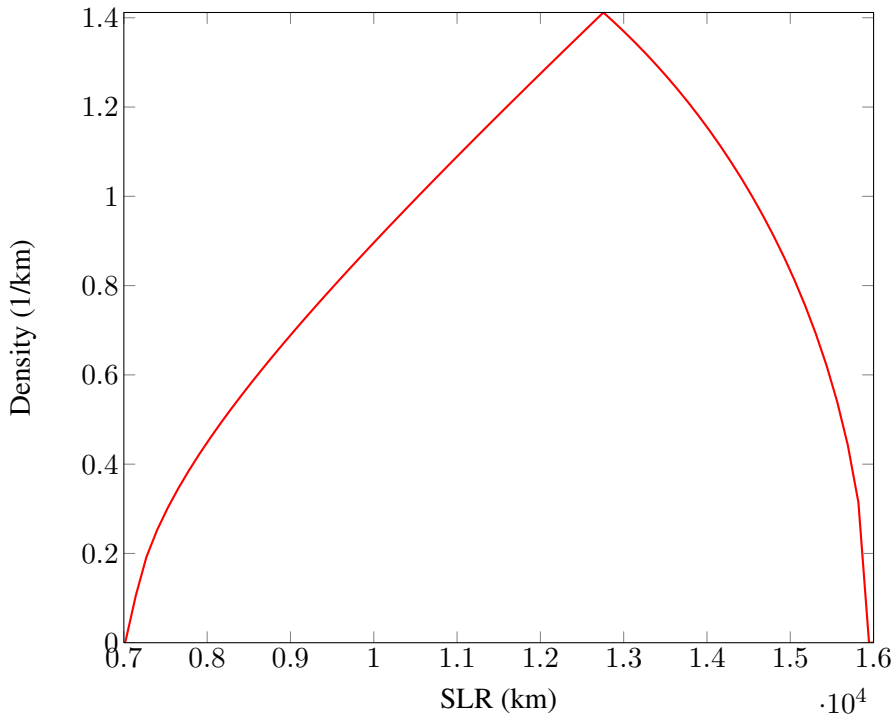

Figure 7. PDF of semilatus rectum from single observation at 8000 km radial distance.

an infinite number of observations uniformly over the part of the orbit that's visible, this sum turns into an integral. Of course, sampled observations will not follow this ideal curve, but do look similar. With more than one orbit (object), it is possible to identify the different orbits and find which one a particular observation more likely belongs to. Of course, this association of observations with orbits is done probabilistically, and those probabilities will change as new observations are made.

To keep this discussion simple, consider only the inclination PDF as discussed previously. In practice, all the elements would be analyzed, and objects close in inclination would differ in other elements (unless they were tethered or formation flying) and thus could be separated when all elements are considered.

Continuous uniform visibility

It is possible mathematically to simulate a single orbit with known inclination and presume uniform observation over the whole orbit, and thereby compute a PDF $\Pr(i|\iota)$, with ι the inclination of the orbit. The position vector in geocentric equatorial coordinates of an orbit with semilatus rectum p, true anomaly θ, etc. is given by

$$\boldsymbol{r} = \mathcal{R}_z(-\Omega)\mathcal{R}_x(-i)\mathcal{R}_z(-\omega)\begin{bmatrix} \frac{p\cos\theta}{1+e\cos\theta} \\ \frac{p\sin\theta}{1+e\cos\theta} \\ 0 \end{bmatrix} \tag{32}$$

with three three-dimension rotations $\mathcal{R}_x$ and $\mathcal{R}_z$. For a circular orbit, this becomes

$$\boldsymbol{r} = \mathcal{R}_z(-\Omega)\mathcal{R}_x(-i)\begin{bmatrix} r\cos u \\ r\sin u \\ 0 \end{bmatrix} \tag{33}$$

with u the argument of latitude, the angle from the node to the observation point. For a circular orbit with inclination ι, the declination as a function of true anomaly is computed from the three components of $\boldsymbol{r}$,

$$\delta_\iota(u) = \arctan\left(\frac{z}{x^2+y^2}\right) = \arctan\left(\frac{\sin\iota\sin u}{\sqrt{\cos^2 u + \cos^2\iota\sin^2 u}}\right). \tag{34}$$

This can be substituted into (5) to get the PDF in inclination for a given value of the true anomaly. That is, the probability density in inclination i, given an observation at argument of latitude u of a circular orbit with inclination ι is

$$\Pr(i|u) = \frac{\sin i}{\pi\sqrt{\cos^2 u + \cos^2\iota\sin^2 u - \cos^2 i}}. \tag{35}$$

The inclination limits (2) can be transformed into limits on u. The declination-inclination relationship

$$\delta = \arctan\left(\frac{\sin\iota\sin u}{\sqrt{\cos^2 u + \cos^2\iota\sin^2 u}}\right) \leqslant i \tag{36}$$

can be rewritten

$$|\sin u| \leqslant \left|\frac{\sin i}{\sin\iota}\right|. \tag{37}$$

In summary, for a circular orbit with inclination ι, the probability density by inclination given a particular the observation at argument of latitude u on that orbit (35) is

$$\Pr(i|u,\iota) = \begin{cases} \dfrac{\sin i}{\pi\sqrt{\cos^2 u + \cos^2\iota\sin^2 u - \cos^2 i}} & \text{if } |\sin u| \leqslant |\sin i/\sin\iota|, \\ 0 & \text{otherwise.} \end{cases} \tag{38}$$

Figure 8 shows a plot for four different inclination values of this PDF integrated over all arguments of latitude ($0 \leqslant u < 2\pi$), and as would be expected, the maximum density occurs at the inclination of the orbit.

Samples from a single orbit

Consider a collection of circular orbits of the same orbital elements (circular, 1000 km altitude, RAAN 0) except for the inclination and mean anomaly. For each chosen value of inclination, the declination of the position vector for each mean-anomaly uniformly sampled is saved as an "observation." The single point PDF (5) is computed from the declination and summed for all observations. This ensemble count distribution from a single orbit with an inclination of 20° is shown in Figure 9. It is not a probability density, because it integrates to the number of samples, not to one. Compare the $\iota = 20°$ curve of Figure 8 with the sampled result shown, keeping in mind that there are 100 samples represented in Figure 9 when looking at the density axis scale.

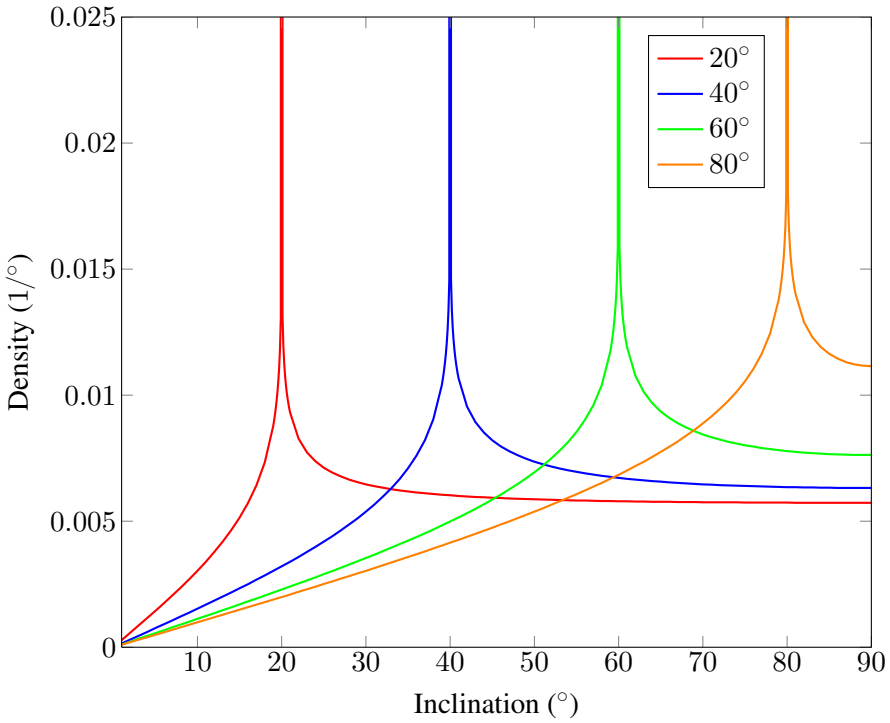

Figure 8. PDF $\Pr(i|\iota)$ for circular orbits of various inclinations ι observed continuously uniformly. The peak values are truncated.

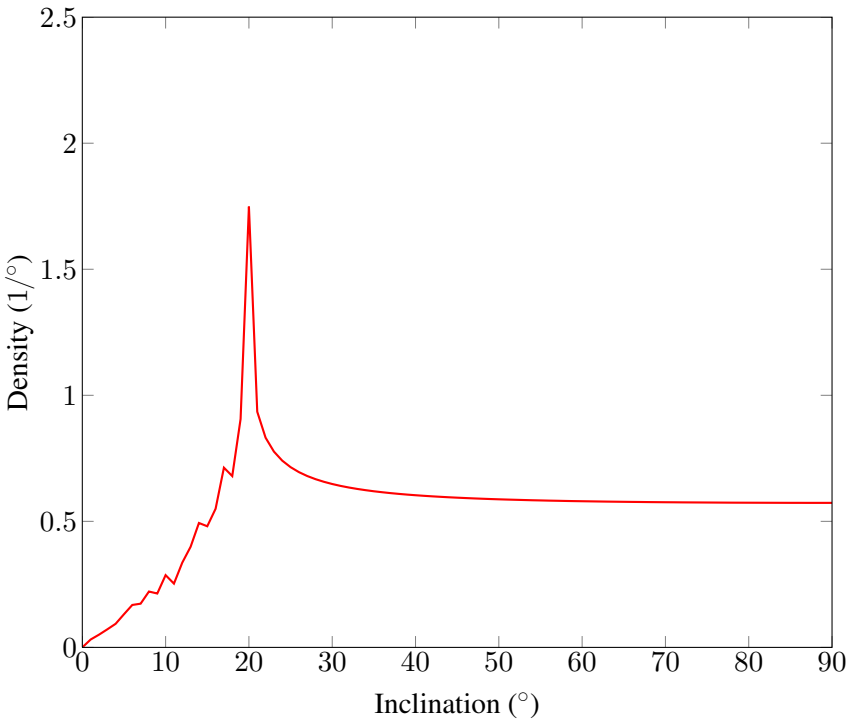

Figure 9. Ensemble count distribution, by inclination, for single orbit with $i = 20°$ and 100 observations.

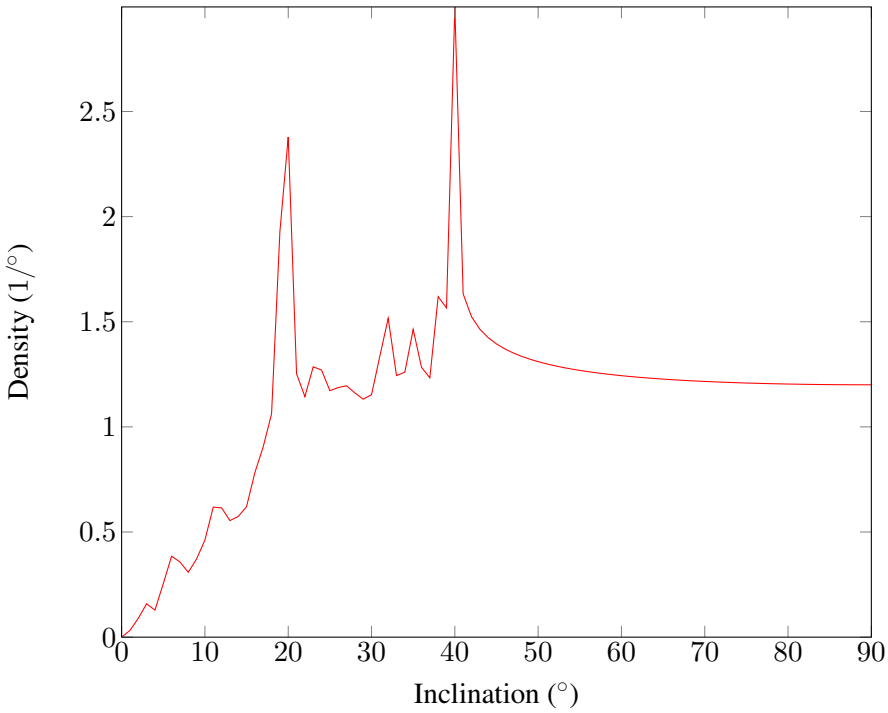

Figure 10. Ensemble count distribution, by inclination, for two orbits with $i = 20^\circ$, $i = 40^\circ$ and 100 observations each.

Samples from multiple orbits

While the observation of declinations from a single orbit gives a clear value of the inclination, the mixture of multiple objects with different orbits into one set of observations is more realistic and complicated. The distribution for two orbits with inclinations of 20° and 40° is shown in Figure 10. It is clear from this plot without knowing the source how many objects there are and what their inclinations are. This is in part due to the sharp rise on the single object PDF for inclination at the declination of the observation, as shown in Figure 2 and the equation (15). Of course, with a more complicated environment that has more orbits with similar inclinations, it would not be as clear. Nevertheless, for the remainder of this paper, it is assumed that the orbits can be identified. The question remains how good the association of a single observation with one of the identified orbits is.

An analysis of this sort is a step on the goal of understanding the orbital population from unassociated observations. Suppose observations of the declination are taken of multiple objects in orbit over a period of time without knowing even how many objects there are or what their orbits are. Is it possible to find out the answer to these questions, and assign an orbit to each of the observations, and how reliably can this be done? The analysis presented offers an initial approach to answering these questions.

Observations may be assigned orbits once the orbits are identified. This can be done in a simple way by picking the orbit whose density is highest for each observation according to the single-observation PDF, say (5) in the case of inclination. The probability of the observation being associ-

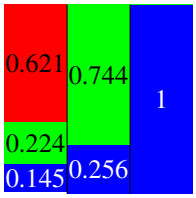

Actual inclination	Identified inclination 20°	40°	60°
20°	100	0	0
40°	36	64	0
60°	25	25	50

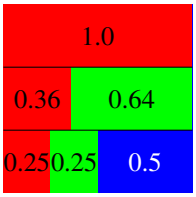

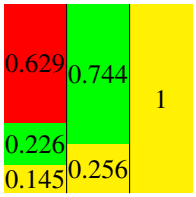

Actual inclination	Identified inclination 20°	40°	80°
20°	100	0	0
40°	36	64	0
80°	23	22	55

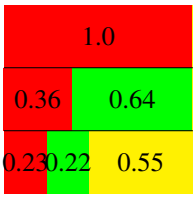

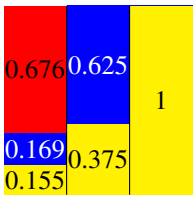

Actual inclination	Identified inclination 20°	60°	80°
20°	100	0	0
60°	25	75	0
80°	23	45	32

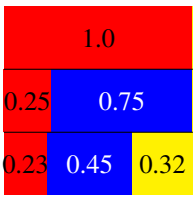

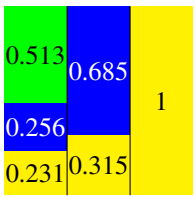

Actual inclination	Identified inclination 40°	60°	80°
40°	100	0	0
60°	50	50	0
80°	45	23	32

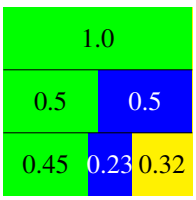

Figure 11. Table of observation association counts and bar plots of posterior (left) and likelihood (right) for three different orbits mixed in an ensemble of observations, with 100 observations of each orbit.

ated with the j^{th} orbit is the ratio of that density to the sum over all the orbits,

$$\Pr(\text{orbit } j|\delta, \{i_k\}) = \frac{\Pr(i_j|\delta, \{i_k\})}{\sum_k \Pr(i_k|\delta, \{i_k\})}. \tag{39}$$

The simplest way to do the assignment is to pick the orbit for which this probability is highest. The analysis proceeds as follows. For each observation, the most likely orbit is selected according to this rule; since we know what orbit that observation corresponds to, we can accumulate the counts in a matrix by actual orbit and identified orbit. In the simulations performed here, there are 100 randomly generated observations for each orbit, and they are the same for each orbit in all the combinations shown.

In Figure 11 all possible sets of three orbits selected from a set of four inclinations ($i = 20^\circ$, $i = 40^\circ$, $i = 60^\circ$, $i = 80^\circ$) are shown. Each combination is shown on a separate line; there is a posterior bar plot on the left, a table of counts in the center, and a likelihood bar plot on the right. The posterior gives the fraction of each of the actual orbits for a given identification of the orbit, and is oriented vertically to reflect the columns in the table. The likelihood gives the fraction of each of the identified orbits for a given actual orbit, and is oriented horizontally to reflect the rows in the table. It is the former, the posterior, that is of greatest interest, because in a real application, the actual orbits will not be known, just the identified orbits.

SUMMARY AND CONCLUSION

No sensor of the orbital environment provides complete orbital state equivalence ($\boldsymbol{r}$ and $\dot{\boldsymbol{r}}$), so satellites must be observed over time to determine orbits. With multiple satellites in orbit, the satellites must be identified so that the observations can be associated to the object. This constitutes a difficult problem when contemplating large numbers of hard-to-distinguish objects, such as small orbital debris. An alternative approach is to consider the unobserved parts of the state to be unknowns with a probability distribution, and use the mechanism of probabilistic inference to conclude (probabilistic) facts about the orbital environment. A single partial-state observation can be used with an uninformative probability density function in the unobserved quantities; for example, the velocity of the satellite for a position-only sensor.

The sure-variable equations of spherical trigonometry and astrodynamics may be represented as probability density functions with some effort. For a position-only observation, the density functions for inclination, right ascension of the ascending node and semilatus rectum can be derived analytically. This assumes an uninformative prior; for the inclination and right ascension of the ascending node, this is the reasonable assumption that all velocity vector directions in the plane perpendicular to $\boldsymbol{r}$ are equally probable. For the semilatus rectum taking the uninformative prior as Cartesian in $\{e\cos\theta, e\sin\theta\}$ is not particularly realistic.

The completion of state from position-only $\boldsymbol{r}$ observation proceeds in two steps. First, the angular momentum direction $\hat{\boldsymbol{h}}$ is chosen as a point on the circle perpendicular to $\boldsymbol{r}$; $\boldsymbol{r}$ and $\hat{\boldsymbol{h}}$ define the orbital plane. Then, the eccentricity vector $\boldsymbol{e}$ in this plane is chosen, which defines the rest of the orbital state. The declination of the observation alone provides the inclination of the orbit, the declination and right ascension of the observation provides the right ascension of the ascending node, and the eccentricity vector defines both e and the true anomaly θ and so defines the two-dimensional orbit.

Posterior probability densities in these orbital elements for a position-only observation may thus be computed analytically. For a single observation with the unrealistic uniform observation assump-

tion, this can be integrated to find an idealized PDF of, say, inclination; as expected, the maximum density is precisely at the orbit's inclination. For multiple observations, the peaks are superimposed, and in some cases can be distinguished by eye, so that the number and elements of orbits may be found. Observations may individually be probabilistically associated with identified orbits.

A simple scheme that compares the probability density of the individual observation at one of the determined orbits' maximum density of the ensemble allows one to assign relative probabilities of the various orbits. Considering simulated ensembles of three different orbit inclinations chosen from a set of four ($i = 20^\circ, 40^\circ, 60^\circ, 80^\circ$), the position-only observation is able to identify orbits with a reliability that ranges from better-than-guessing (up to 2/3) for the lower orbits, to certainty ($p = 1$) for the highest orbit.

This result is very preliminary, but shows promise for more research and application to unassociated observation data. It includes only one orbital element, inclination; when other elements are included, the ability to separate orbits and associate observations should improve. On the other hand, there is no realistic sampling from an earth-fixed observer; the assumption has been made that the satellites are observed uniformly over their orbits, which is not a reasonable assumption.

APPENDIX: CHANGE OF VARIABLES

The principle mathematical tool needed in the computation of posterior PDFs is the change of variables (sometimes called "propagation of errors"). While this sounds straightforward, it can in fact be very complex; see Sivia and Skilling.[9] Fortunately, for univariate differentiable functions, the formula is not too complicated, and the function we use in this paper are of this type. The transformation $g : X \to Y$ of a univariate PDF f in the random variable X is given by*

$$\sum_k \left| \frac{d}{dy} g_k^{-1}(y) \right| f_X\left(g_k^{-1}(y)\right), \tag{40}$$

with the sum over all inverse images of the value y. If the function is monotonic, the sum will be of one term only. This involves not only a calculation of the derivative, but a substitution of variables from the inverse image, since the function should be in x only and not y.

REFERENCES

[1] E. T. Jaynes, *Probability Theory: The Logic of Science*. Cambridge, UK: Cambridge, 2003.

[2] E. L. Woollett, *Maxima by Example*. San Luis Obispo, CA: Woollett, 2012. http://www.csulb.edu/~woollett/#mbe. URL: http://www.csulb.edu/~woollett/#mbe.

[3] R. M. Weisman, M. Majji, and K. T. Alfriend, "Analytic characterization of measurement uncertainty and initial orbit determination on orbital element uncertainty and correlation," *Spaceflight Mechanics 2013* (S. Tanygin, R. S. Park, T. F. S. Jr., and L. K. Newman, eds.), Vol. 148 of *Advances in the Astronautical Sciences*, San Diego, California, Univelt, Inc., 2013, pp. 37–56. Paper AAS 13–203.

[4] R. M. Weisman, M. Majji, and K. T. Alfriend, "Application of the Transformation of Variables Technique for Uncertainty Mapping in Nonlinear Filtering," *Astrodynamics 2011* (H. Schaub, B. C. Gunter, R. P. Russell, and W. T. Cerven, eds.), Vol. 142 of *Advances in the Astronautical Sciences*, San Diego, California, Univelt, Inc., 2011, pp. 3129–3148. Paper AAS 11–604.

[5] C. Binz and L. Healy, "Utilization of Uncertainty Information in Angles-Only Initial Orbit Determination," *Spaceflight Mechanics 2014*, Advances in the Astronautical Sciences, San Diego, CA, American Astronautical Society, Univelt, Inc., January 2014. Paper 14–431.

[6] D. A. Vallado, *Fundamentals of Astrodynamics and Applications*, Vol. 12 of *The Space Technology Library*. El Segundo, California and Dordrecht, The Netherlands: Microcosm Press and Kluwer Academic Publishers, second ed., 2001.

*https://en.wikipedia.org/wiki/Probability_density_function

[7] M. Walker, B. Ireland, and J. Owens, "A set of modified equinoctial orbit elements," *Celestial Mechanics*, Vol. 36, 1985, pp. 409–419, 10.1007/BF01227493.

[8] B. V. K. V. Kumar, A. Mahalanobis, and R. D. Juday, *Correlation pattern recognition*. Cambridge, UK: Cambridge University Press, 2005.

[9] D. S. Sivia and J. Skilling, *Data Analysis: A Bayesian Tutorial*. Oxford University Press, second ed., 2010.